Chapter 4

Fluorescent Biosensors for the Detection of HMGB1 Release

Isabelle Martins, Oliver Kepp, Laurie Menger, Mickäel Michaud, Sandy Adjemian, Abdul Qader Sukkurwala, Erika Vacchelli, Lorenzo Galluzzi, and Guido Kroemer

Abstract

During necrosis and following some instances of apoptosis (in particular in the absence of a proficient phagocytic system), the nonhistone chromatin component high-mobility group box 1 (HMGB1) is released in the extracellular space. In vivo, extracellular HMGB1 can bind Toll-like receptor 4 on the surface of dendritic cells, de facto operating as a danger-associated molecular pattern and alarming the organism to the presence of stressful conditions. Recent results indicate that the release of HMGB1 is one of the key features for cell death to be perceived as immunogenic, i.e., to be capable of triggering a cognate immune response in vivo. Thus, only anticancer agents that—among other features—allow for the release of HMGB1 as they induce cell death are expected to stimulate anticancer immune responses. To investigate the immunogenic potential of conventional anticancer agents and novel cell death inducers on a high-throughput scale, we engineered human osteosarcoma U2OS cells to express HMGB1 fused at the N-terminus of the green fluorescent protein (GFP). Coupled to fluorescence microscopy workstations for automated image acquisition and analysis, this HMGB1-GFP-based biosensor is amenable for the identification of potential inducers of immunogenic cell death among large chemical libraries.

Key words ATP, Autophagy, Cancer, Calreticulin, Hoechst 33342, Pyknosis

1 Introduction

For a long time, necrosis has been considered as a purely accidental cell death mode, and was operationally defined by the absence of morphological traits of apoptosis and autophagy [1, 2]. Thus, until a few years ago, necrosis was viewed as a totally uncontrollable process, featuring the early breakdown of the plasma membrane followed by a rather disorganized degradation/release of the intracellular content [3]. Recently, it has become clear that—similar to apoptosis—primary necrosis can be regulated, in both its occurrence and its course [4]. This has stimulated an intense wave of investigation on the signaling pathways that underpin regulated necrosis [5–7]. In addition, accumulating evidence indicates that regulated necrosis plays a critical role in multiple physiological and

Kimberly McCall and Charles Klein (eds.), *Necrosis: Methods and Protocols*, Methods in Molecular Biology, vol. 1004,
DOI 10.1007/978-1-62703-383-1_4,

pathological settings [8–10], de facto generating interest in the discovery/development of chemicals that would specifically activate or inhibit regulated necrosis. Inducers of regulated necrosis would indeed constitute promising anticancer agents, in particular for the therapy of chemorefractory (which near-to-always means apoptosis-resistant) tumors. Conversely, inhibitors of the signaling pathways that drive regulated necrosis would be particularly useful for avoiding unwarranted cell death in multiple pathophysiological settings, including ischemia and viral infection [11]. These recent developments in the field of cell death research have raised the need for cell death assays that specifically detect (regulated) necrosis on a high-throughput basis.

Primary necrosis can be accidental (such as in the case of cells succumbing to very harsh environmental conditions like freeze–thaw cycles) or regulated (such as that ignited by the ligation of some death receptors in conditions in which caspase-8 cannot be activated). In addition, necrosis can ensue apoptosis (as well as other cell death subroutines) [12], especially in vitro or in the absence of a proficient phagocytic system [13]. In this setting, which is known as secondary necrosis, apoptotic bodies that are not properly cleared by phagocytic cells progressively lose their integrity, eventually allowing for the spillage of intracellular contents into the extracellular milieu [13]. Importantly, primary necrosis (be it accidental or regulated) and secondary necrosis converge on similar cellular disintegration features [14], implying that end-stage determinations are inappropriate for discriminating among these mechanistically distinct cell death modes. Similar considerations can be made for the early stages of these catabolic processes: most of the biochemical features that characterize the activation and execution of regulated necrosis (e.g., mitochondrial and lysosomal membrane permeabilization, abrupt ATP consumption, overgeneration of reactive oxygen species by mitochondria and non-mitochondrial sources, cytosolic Ca^{2+} overload, activation of non-caspase proteases) can be detected in instances of apoptotic cell death and accidental necrosis [3, 5]. Thus, current techniques for discriminating primary necrosis from post-apoptotic secondary necrosis are all based on kinetic determinations [3].

One common approach in this sense is based on the detection of plasma membrane integrity. Indeed, whereas apoptotic cells and apoptotic bodies retain intact plasma membranes for relatively long periods (in the range of hours–days), cells succumbing to primary necrosis rapidly undergo plasma membrane permeabilization [3, 7]. Several methods have been developed to follow the permeabilization of plasma membranes, including techniques based on the uptake by dying cells of exclusion dyes (i.e., compounds that enter cells only when the integrity or their membrane is compromised) as well as protocols based on the

detection in the extracellular milieu of non-secreted intracellular proteins, including lactate dehydrogenase (LDH) and high-mobility group box 1 (HMGB1) [3, 15].

LDH has been extensively used to monitor plasma membrane breakdown as it is enzymatically active, which largely facilitates colorimetric detection [5, 15]. HMGB1 is a nonhistone chromatin component involved in transcriptional regulation but devoid of enzymatic activity [16]. Irrespective of this, the quantification of extracellular HMGB1 with commercially available ELISA-based kits has become a routine approach for monitoring necrosis, presumably due to the fact that extracellular HMGB1 has been recognized as a potent pro-inflammatory agent [16–18], and hence intimately (though incorrectly, at least in part) associated with necrosis. Recent data indicate indeed that HMGB1 is released not only following necrosis but also in some instances of apoptosis [19], arguing against the use of extracellular HMGB1 as a necrosis-specific marker.

However, as the interaction between HMGB1 and Toll-like receptor 4 (TLR4) has been shown to be one of the key features of immunogenic cell death (ICD) [20, 21], the interest in monitoring the release of HMGB1 has not vanished, but only changed focus. Thus, extracellular HMGB1 is now being used as a surrogate marker of the immunogenic potential of chemotherapeutic agents and other cell death inducers. Importantly, the release of HMGB1 is required, but not sufficient, for cell death to be perceived as immunogenic, implying that other parameters must be monitored to confirm the ability of specific compounds to trigger ICD [20]. In this setting, in vivo vaccination tests remain the gold standard method for determining the true immunogenic potential of putative ICD inducers [22]. This said, the detection of HMGB1 release on a high-throughput basis might constitute a reliable and relatively inexpensive tool to perform primary screens on large chemical libraries for the identification of ICD inducers.

Commercial kits for the ELISA-based end-point quantification of HMGB1 in culture supernatants (and body fluids) are relatively inappropriate for this aim, as they are intrinsically unable to monitor the dynamic aspects of HMGB1 release. To circumvent this issue while maintaining the possibility to perform end-point determinations, we engineered human osteosarcoma U2OS cells to express HMGB1 fused at the N-terminus of the green fluorescent protein (GFP) and developed a fluorescence microscopy-based automated method for the high-throughput analysis of HMGB1 release. It should be noted that the immunodetection of HMGB1 was not an option for our aims. Indeed, cells that release HMGB1 are in the late steps of the cell death program, and hence prone to detach from the substrate. In this context, minimizing the number of washing steps represents *a conditio sine qua non* for avoiding an excessive loss of cells from samples, rendering immunofluorescence microscopy-based techniques incompatible with this approach.

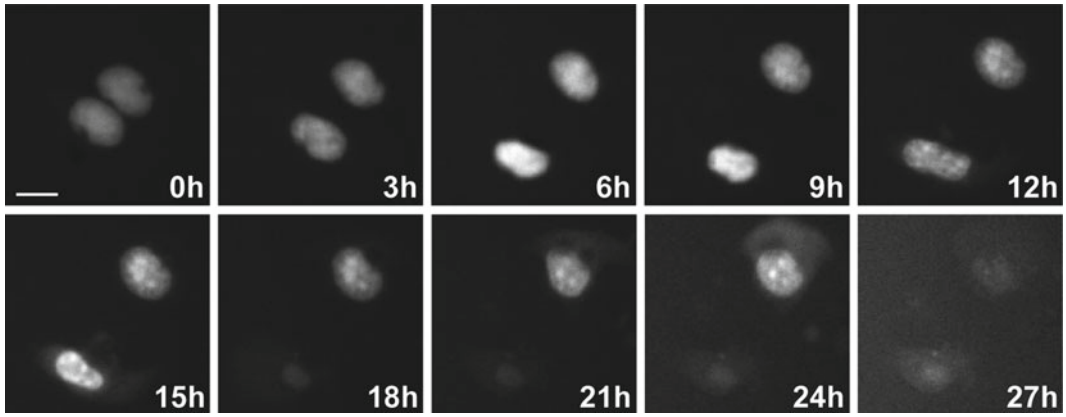

Fig. 1 Release of HMGB1 in the context of immunogenic cell death. Human osteosarcoma U2OS cells stably expressing a HMGB1-GFP fusion protein were treated with 2 μM mitoxantrone (MTX) and then green fluorescence was monitored by videomicroscopy for a total time of 27 h. Representative snapshots are depicted. Scale bar = 10 μm. Please note the progressive loss of the nuclear green signal, paralleled by an increase in extracellular fluorescence

To provide a proof of principle for our approach, we first treated U2OS cells stably expressing HMGB1-GFP with the prototypic ICD inducer mitoxantrone (MTX) and followed by the release of HMGB1 by videomicroscopy (Fig. 1). Then, we tested HMGB1 release on fixed samples. To this aim, U2OS cells stably expressing HMGB1-GFP were left untreated or treated with MTX for 24 or 48 h, followed by fixation and nuclear counterstaining with the chromatinophilic dye Hoechst 33342. This additional step was undertaken as it facilitates the generation of regions of interest (ROIs) by the software for automated image analysis (Fig. 2), hence facilitating the processing of large amount of images. Of note, while the majority of untreated cells retained HMGB1 in the nucleus (Fig. 3a), MTX induced HMGB1 release in a vast proportion of cells, concomitant with morphological signs of apoptosis (nuclear shrinkage) (Fig. 3b).

The fluorescent biosensor that we describe here is amenable to the kinetic analysis of HMGB1 release in a high number of samples, de facto being compatible with large drug screening campaigns and genome-wide siRNA-based screens.

2 Materials

2.1 Common Materials

2.1.1 Disposables

1. 96-well black/clear, poly-L-lysine-treated plates, flat bottom with lid.
2. 1.5 mL microcentrifuge tubes.
3. 15 and 50 mL conical centrifuge tubes.
4. 25, 75, or 175 cm^2 flasks for cell culture.
5. 6-, 12-, and 96-well plates for cell culture.

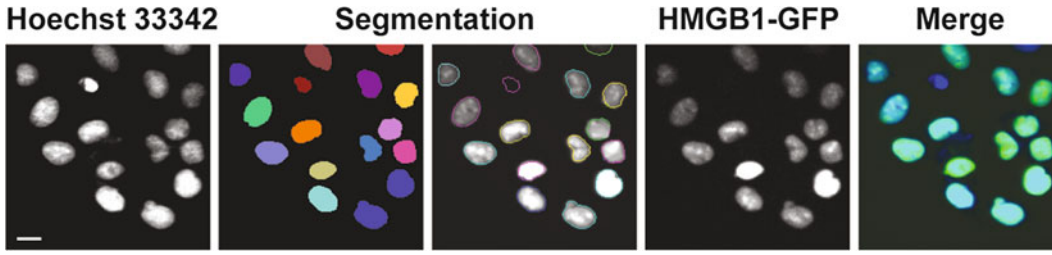

Fig. 2 Image segmentation for the definition of regions of interest (ROIs). Human osteosarcoma U2OS cells stably expressing a HMGB1-GFP fusion protein were maintained in culture conditions for 24 h, then fixed, and counterstained with Hoechst 33342 as described in Subheading 3.3, **step 3**. Images captured with the BD Pathway 855 workstation are automatically treated to generate ROIs based on the Hoechst 33342 signal. This segmentation mask allows the software to identify nuclei, and hence to decipher the localization of HMGB1-GFP in merged images. Scale bar = 10 μm

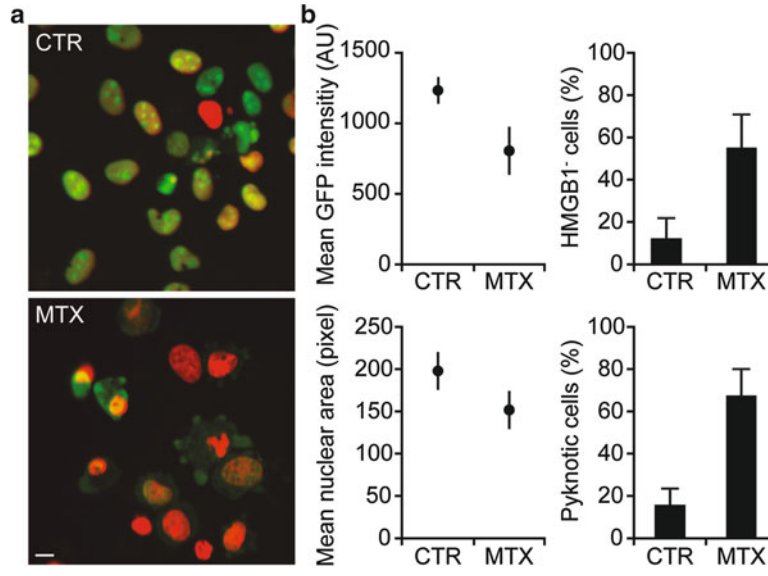

Fig. 3 Quantitative assessment of HMGB1 release. Human osteosarcoma U2OS cells stably expressing a HMGB1-GFP fusion as well as a H2B-RFP chimera were maintained in control conditions (CTR) or treated with 2 μM mitoxantrone (MTX) for 24 h. Thereafter, cells were processed for the automated detection of HMGB1 release as described in Subheading 3.3, **steps 3–5**. In panel (**a**), representative images are reported (scale bar = 10 μm). Panel (**b**) depicts quantitative data (mean ± SEM, $n = 4$ viewfields containing at least 250 cells each, triplicate independent determinations)

2.1.2 Equipment

1. Bright-field inverted microscope: XDS-1R (Optika, Ponteranica, Italy), equipped with 10×, 25×, and 40× long working distance planachromatic objectives.
2. Automated imaging workstation: Pathway 855 (BD, San José, USA), equipped with a 20× UApo/340 apochromatic objective with 0.75 numerical aperture (Olympus, Tokyo, Japan), Photofluor II light sources (Chroma, Rockingham, USA), an ORCA-AG Deep Cooled Digital Camera (Hamamatsu Photonics, Hamamatsu, Japan), and appropriate excitation/emission filter sets (Semrock, Rochester, USA).
3. Cell sorter: FACSVantage (BD), equipped with a UV laser and a 70 μm nozzle, in association with the operational/analytical software CellQuest™ Pro (BD).

2.1.3 Reagents

1. Complete growth medium for U2OS cells: Dulbecco's modified essential medium (DMEM) containing 4.5 g/L glucose, L-glutamine, and pyruvate, supplemented with 100 mM HEPES buffer, 1× nonessential amino acids, 100 U/mL penicillin G (sodium salt), 100 μg/mL streptomycin sulfate, and 10 % fetal bovine serum (FBS) (*see* **Note 1**).
2. Phosphate-buffered saline (PBS, 1×): 137 mM NaCl, 2.7 mM KCl, 4.3 mM Na_2HPO_4, 1.4 mM KH_2PO_4 in deionized water (dH_2O), adjust pH to 7.4 with 2 N NaOH.
3. Trypsin/EDTA: 0.25 % trypsin–0.38 g/L (1 mM) EDTA×4 Na^+ in Hank's Balanced Salt Solution (HBSS, Sigma), stored at –20 °C (*see* **Notes 2** and **3**).
4. Alignment beads: AlignFlow™ Plus flow cytometry alignment beads, Ø = 6 μm, for 350–370 nm and 488 nm excitation (Molecular Probes-Life Technologies, Grand Island, USA), stock solution at 1.2×10^8 beads/mL, stored at 4 °C under protection from light (*see* **Notes 4** and **5**).
5. Sheath fluid: FACSFlow™ (BD), stored at room temperature (RT) (*see* **Note 6**).

2.2 Generation of HMGB1-GFP-Expressing U2OS Cells

1. G418 sulfate (geneticin), stock solution at 50 mg/mL, stored at –20 °C (*see* **Notes 7–9**).
2. pGFP-N1 (Clonetech Laboratories Inc, Mountain View, USA) with HMGB1 inserted in the *EcoR*I/*Sac*II site (pHMGB1-GFP), stock solution in dH_2O, 1 mg/mL, stored at –20 °C (*see* **Note 10**).
3. Lipofectamine™ 2000 transfection reagent (Invitrogen-Life Technologies), stored at 4 °C (*see* **Note 11**).
4. Opti-MEM®-I reduced serum medium supplemented with phenol red (Gibco-Life Technologies), stored at 4 °C (*see* **Note 11**).

2.3 Characterization of HMGB1 Release by Automated Microscopy

1. Phenol red-free DMEM containing 4.5 g/L glucose, L-glutamine, and pyruvate, supplemented with 25 mM HEPES buffer and 1× nonessential amino acids.
2. 2 mM MTX (Sigma-Aldrich, St. Louis, USA), stock solution in dH_2O, stored at 4 °C under protection from light and in tightly sealed containers (*see* **Notes 12** and **13**).
3. 10 mg/mL Hoechst 33342 (Molecular Probes-Life Technologies), stock solution in dH_2O, stored at 4 °C under protection from light (*see* **Notes 14** and **15**).
4. Fixative solution: 8 % paraformaldehyde (PFA), supplemented with 4 mg/mL Hoechst 33342 (w/v in PBS) solution (*see* **Notes 16** and **17**).

3 Methods

3.1 Cell Culture

1. Upon thawing, U2OS cells are routinely maintained in complete growth medium in 75–175 cm^2 flasks (37 °C, 5 % CO_2) (*see* **Note 18**).
2. When confluence approaches 70–90 %, cells are detached with trypsin/EDTA (*see* **Notes 19–22**) to constitute fresh maintenance cultures (*see* **Notes 23** and **24**) and to provide cells for experimental determinations.
3. The latter are carried out in 6-well standard or 96-well imaging plates, according to the specific experimental setting.

3.2 Generation of HMGB1-GFP-Expressing U2OS Cells

1. 2×10^5 U2OS cells are seeded in 6-well plates (in 2 mL growth medium per well) and allowed to adhere for 12–24 h (*see* **Notes 25** and **26**).
2. Transfection complexes are generated as follows (conditions on a per well basis):
   (a) 3 μL Lipofectamine™ 2000 transfection reagent are diluted in 50 μL pre-warmed Opti-MEM®-I.
   (b) Meanwhile, 1.5 μg pHMGB1-EGFP are dissolved in 50 μL pre-warmed Opti-MEM®-I.
   (c) After 5 min of incubation at RT, the plasmid and Lipofectamine™ 2000 solutions are combined (total volume = 100 μL), gently mixed, and kept for further 15–20 min at RT (*see* **Notes 27** and **28**).
3. While transfection complexes form, complete growth medium is substituted with serum-free medium (1 mL per well) (*see* **Note 29**).
4. When complex formation is over, 100 μL transfection complexes are added dropwise to each well, and plates are gently

whirled and kept in standard culture conditions (37 °C, 5 % CO_2) for 4–6 h (*see* **Note 30**).

5. Standard culture conditions are reestablished by the addition of complete growth medium supplemented with 30 % FBS (500 μL per well) (*see* **Note 31**).
6. The next day, cells are detached and reseeded in 6- or 12-well plates, in complete growth medium supplemented with 1 mg/mL G418 (*see* **Notes 19–22**).
7. HMGB1-GFP-expressing clones are sorted in sterile conditions by FACS (1 cell/well in 96-well plates, in 200 μL complete growth medium) or by the limiting dilution technique (0.1, 1, and 3 cells/well in 96-well plates; in 200 μL complete growth medium) (*see* **Notes 32–35**).
8. Following 7–10 days of culture in standard conditions (*see* **Note 36**), HMGB1-GFP-expressing clones are visually identified by fluorescence microscopy-assisted inspection.
9. Selected clones are amplified and several aliquots for use and long-term storage in liquid nitrogen are generated starting from a homogenous and healthy population (*see* **Note 37**).

3.3 Characterization of HMGB1 Release by Automated Microscopy

1. $0.5–1 \times 10^3$ HMGB1-GFP-expressing U2OS cells (*see* Subheading 3.2) are seeded in 100 μL phenol red-free growth medium in 96-well imaging plates and let adapt for 12–24 h (*see* **Note 25**).
2. Thereafter, cells are treated with the compounds of choice previously diluted (3×) in 50 μL complete growth medium. As a positive control, 1–4 μM (final concentration) MTX can be employed.
3. Upon incubation for the time of choice (*see* **Note 38**), 50 μL of fixative solution (*see* **Note 39**) are gently added to each well.
4. Images (4 viewfields/well, to ensure a minimum of 250 cells per experimental condition) are acquired by the automated workstation and data stored on an external server prior to analysis (*see* **Note 40**).
5. Analysis includes:
   (a) The generation of ROIs based on automatically thresholded Hoechst 33342 signal (identifying nuclei) (*see* **Notes 41–43**).
   (b) The calculation of mean GFP fluorescence intensity in each ROI, defining the presence/absence of nuclear HMGB1 (*see* **Note 44**).
   (c) The estimation of nuclear area, as an indicator of apoptotic nuclear shrinkage (*see* **Note 45**).

4 Notes

1. Optimal growth conditions (e.g., medium composition, supplements) vary according to the cell line of choice, and may quite dramatically influence not only growth rates but also the response to cell death inducers. For this reason, we suggest to use the medium that is most suitable for the cell line of choice, as recommended by the American Type Culture Collection (ATCC, Manassas, USA).
2. Appropriately stored (–20 °C, under protection from light), trypsin–EDTA is stable for at least 18 months.
3. EDTA is not currently listed as a carcinogen by the National Toxicology Program (NTP), the International Agency for Research on Cancer (IARC), or the Occupational Safety and Health Administration (OSHA).
4. AlignFlow™ Plus flow cytometry alignment beads are provided as suspensions in water containing 0.05 % Tween 20 and 2 mM sodium azide (NaN_3). Tween 20 is not currently listed as a carcinogen by NTP, IARC, or OSHA, yet may behave as a mild irritant for the eyes, skin, and respiratory system. NaN_3 is toxic by ingestion and under acidic conditions may release the highly toxic gas hydrazoic acid.
5. Appropriately stored (4 °C, under protection from light) AlignFlow™ Plus flow cytometry alignment beads are stable for at least 12 months.
6. FACSFlow™ is a mixture of multiple substances, any of which, at their given concentration, and is considered to be hazardous to health.
7. Geneticin is a nucleoside antibiotic isolated from *Micromonospora rhodorangea*, which inhibits protein synthesis in both prokaryotic and eukaryotic cells.
8. Geneticin is toxic, if swallowed, and should always be handled using protective gloves, clothing, and eyewear.
9. When stored properly at –20 °C, geneticin is stable for up to 9 months. Media supplemented with geneticin can be stored at 4 °C for up to 2 weeks. The manufacturer recommends avoiding repetitive freezing and thawing of the antibiotic.
10. pHMGB1-GFP is designed for stable expression in mammalian cells of a human HMGB1-GFP chimera driven by the strong pCMV promoter. This vector also contains a cassette encoding G418 resistance for the selection of transfected cells.
11. Lipofectamine™ 2000 and Opti-MEM®-I are generally considered as nonhazardous.

12. MTX is a cytostatic anthracenedione that intercalates in DNA and increases the incidence of double-strand breaks by stabilizing the cleavable complex of topoisomerase II and DNA. MTX is currently used as a chemotherapeutic agent against leukemia and solid tumors.
13. MTX is toxic and a potential carcinogen for humans. This compound may cause heritable genetic damage, and harm to the unborn child, and may be harmful if inhaled, swallowed, or absorbed through skin. Therefore, MTX should always be handled with care by using protective gloves, clothing, and eyewear.
14. Hoechst 33342 is a DNA-intercalating agent currently listed among substances that may cause concern to man owing to possible mutagenic effects but for which the available information is inadequate for making satisfactory assessments. This DNA dye should be handled anyway with the maximal care, by using protective gloves, clothing, and eyewear.
15. As compared to other chromatinophilic dyes (e.g., 4′,6-diamidino-2-phenylindole dihydrochloride, DAPI), Hoechst 33342 is particularly prone to photobleaching. Exposure to light of the stock solution should therefore be carefully prevented.
16. PFA is very toxic by inhalation and should be handled with maximal care under an appropriate chemical fume hood.
17. As the stability of PFA in solution is limited, it should be prepared immediately before use. Upon preparation, the solution should be kept on ice throughout the duration of the experiment.
18. It is recommendable to allow freshly thawed cells to re-adapt for 2–3 passages before using them in experimental assessments. Similarly, it is good practice to define a maximal number of passages and to discard maintenance cultures once this limit has been reached, to avoid genetic population drifts. This strategy requires an appropriate liquid nitrogen stock of cells, which should be generated from a homogenous and healthy population before the beginning of the experiments.
19. Three milliliter and 5–6 mL trypsin/EDTA are largely sufficient for the detachment of cells from 75 to 175 cm^2 flasks, respectively. 300 μL and 1 mL trypsin/EDTA per well should be used for 12- and 6-well plates, respectively (*see* also **Notes 2** and **3**).
20. Before the addition of trypsin/EDTA, adherent cells should be washed once with pre-warmed, sterile PBS. This step facilitates the subsequent trypsinization by minimizing the amount of FBS (which inactivates trypsin) within the flask.

21. Trypsinization time is a function of cell type, viability, and culture density. For U2OS cells (and most cell lines), 5 min at 37 °C are amply sufficient to fully detach a totally confluent, healthy population. It is however recommendable to check for complete cell detachment by visual inspection or by rapid observation in light microscopy.
22. Trypsinization-resistant cells can be mechanically detached with the help of a common scraper for cell culture.
23. For maintenance, U2OS cells can be split at 1:4–1:20 ratios, according to the experimental needs. Other cell lines are more sensitive and may have problems in recovering a normal growth rate if excessively diluted.
24. An alternative to 75 cm^2 flasks is provided by 10 cm Ø Petri dishes. These are equal in surface to 75 cm^2 flasks but more accessible, which can be advantageous if cells need to be detached by scraping (*see* also **Note 22**).
25. Normally, U2OS cells quickly adhere to cell culture supports and hence do not need prolonged adaptation times. This may not hold true for other cell types (e.g., colon carcinoma HCT 116 cells), which should always be allowed to adapt for 24–36 h prior to any experimental manipulation.
26. Both over- and underconfluence are associated with poor transfection rates, the former due to limited uptake of transfection complexes, and the latter because of liposome-mediated toxicity (which is favored when the cell:Lipofectamine™ 2000 ratio is low). For this reason, cell density at transfection should range between 70 and 80 %.
27. When diluted Lipofectamine™ 2000 and the plasmid DNA are mixed, the solution may become cloudy.
28. Liposome-mediated plasmid transfection is carried out entirely at RT under a common safety cabinet. However, it is recommendable to keep the tubes containing plasmid stocks and the Lipofectamine™ 2000 reagent on ice (and to return them to storage conditions immediately after use), in order to minimize solvent evaporation and avoid liposome degradation.
29. For easily transfectable cell lines (e.g., HeLa cells), complete growth medium (including FBS and antibiotics) can be used instead of serum-free culture medium.
30. To avoid intra-well variations of transfection efficiency as well as local toxicity, transfection complexes (which exhibit a very high affinity for plasma membranes) should be added to cells very slowly and dropwise while trying to cover the whole surface of the growth medium.
31. As an alternative, the transfection medium can be discarded and substituted with fresh complete growth medium.

32. As geneticin-resistant cells may appear independent of transfection, we recommend to perform FACS-assisted sorting and selection of GFP^+ cells as soon as possible (transgene expression should be detectable as soon as 12–24 h after transfection). In this context, the use of GFP^- parental cells is required for the identification of GFP-dependent fluorescence.
33. Wild-type GFP is characterized by absorption/emission peaks at 475/508 nm.
34. Perform cell sorting upon gating on events exhibiting normal light-scattering parameters (forward and side scatter, i.e., FSC and SSC, respectively). As a reminder, while FSC depends on cell size, SSC reflects the refractive index, which in turn is influenced by multiple parameters including cellular shape and intracellular complexity (i.e., presence of cytoplasmic organelles and granules).
35. The use of three cell seeding concentrations maximizes the cloning efficiency of the limiting dilution approach.
36. To further reduce the possibility that HMGB1-GFP^- cells might take over cultures, geneticin selection should never be discontinued.
37. It is recommendable to confirm HMGB1-GFP expression by fluorescence microscopy shortly before the generation of vials for long-term storage and use. Along similar lines, cells should be tested for the presence of common laboratory contaminants (e.g., *Mycoplasma spp*).
38. Optimal incubation times are a function of both the cell type and the compound of choice. As a guideline, MTX induces optimal HMGB1 release by U2OS cells in 24–48 h.
39. Upon fixation and if appropriately conserved (4 °C, under protection from light), plates are stable for no more than 2 months.
40. The use of an external, high-capacity server for data storage is highly recommended, as the automated imaging workstation generates very large file sets. As a guideline, the imaging of a 96-well plate at a single time-point, 4 viewfields/well, generates approximately 1 Gb of data.
41. Hoechst 33342 is a cell-permeant chromatinophilic dye (absorption/emission peaks = 352/461 nm) that optimally binds to DNA at pH 7.4. Unbound Hoechst 33342 has an emission peak in the 510–540 nm range (green). This fluorescence can be observed when excessive Hoechst 33342 concentrations are employed.
42. ROI-based image segmentation de facto identifies portions of the images that correspond to single cells, hence allowing the software to perform all subsequent determinations on a per cell basis.

43. To avoid the use of Hoechst 33342 for nuclear counterstaining, cells can be further engineered to express a histone 2B-red fluorescent protein (H2B-RFP) fusion, de facto labeling nuclear chromatin in red. TurboRFP, one among many RFP variants that are currently available, is characterized by absorption/emission peaks at 533/574 nm.
44. The intensity of the GFP signal within each ROI allows the software to determine whether HMGB1 is still localized to the nucleus (co-localization with the Hoechst 33342 signal) or whether it has been released.
45. Together with the GFP signal, nuclear area, as identified by the number of pixel positive for Hoechst 33342, can be employed to assess whether HMGB1 has been released before or after chromatin condensation (which normally is a late event of apoptosis).

Acknowledgment

We thank Dr. Ilio Vitale (INSERM U848, Villejuif France) for his help with manuscript preparation. GK is supported by the Ligue Nationale contre le Cancer (Equipe labellisée), Agence Nationale de la Recherche (ANR), Cancéropôle Ile-de-France, Fondation pour la Recherche Médicale (FRM), Institut National du Cancer (INCa), European Commission (Active p53, Apo-Sys, RIGHT, TransDeath, ChemoRes, ApopTrain), Fondation pour la Recherche Médicale (FRM), and the LabEx Immuno-Oncology.

References

1. Galluzzi L, Maiuri MC, Vitale I, Zischka H, Castedo M, Zitvogel L, Kroemer G (2007) Cell death modalities: classification and pathophysiological implications. Cell Death Differ 14:1237–1243
2. Kroemer G, Galluzzi L, Vandenabeele P, Abrams J, Alnemri ES, Baehrecke EH, Blagosklonny MV, El-Deiry WS, Golstein P, Green DR, Hengartner M, Knight RA, Kumar S, Lipton SA, Malorni W, Nunez G, Peter ME, Tschopp J, Yuan J, Piacentini M, Zhivotovsky B, Melino G (2009) Classification of cell death: recommendations of the Nomenclature Committee on Cell Death 2009. Cell Death Differ 16:3–11
3. Kepp O, Galluzzi L, Lipinski M, Yuan J, Kroemer G (2011) Cell death assays for drug discovery. Nat Rev Drug Discov 10:221–237
4. Golstein P, Kroemer G (2007) Cell death by necrosis: towards a molecular definition. Trends Biochem Sci 32:37–43
5. Galluzzi L, Vitale I, Abrams JM, Alnemri ES, Baehrecke EH, Blagosklonny MV, Dawson TM, Dawson VL, El-Deiry WS, Fulda S, Gottlieb E, Green DR, Hengartner MO, Kepp O, Knight RA, Kumar S, Lipton SA, Lu X, Madeo F, Malorni W, Mehlen P, Nunez G, Peter ME, Piacentini M, Rubinsztein DC, Shi Y, Simon HU, Vandenabeele P, White E, Yuan J, Zhivotovsky B, Melino G, Kroemer G (2012) Molecular definitions of cell death subroutines: recommendations of the Nomenclature Committee on Cell Death 2012. Cell Death Differ 19:107–120
6. Galluzzi L, Kroemer G (2008) Necroptosis: a specialized pathway of programmed necrosis. Cell 135:1161–1163
7. Vandenabeele P, Galluzzi L, Vanden Berghe T, Kroemer G (2010) Molecular mechanisms of necroptosis: an ordered cellular explosion. Nat Rev Mol Cell Biol 11:700–714

8. Vanlangenakker N, Vanden Berghe T, Krysko DV, Festjens N, Vandenabeele P (2008) Molecular mechanisms and pathophysiology of necrotic cell death. Curr Mol Med 8:207–220
9. Vanlangenakker N, Vanden Berghe T, Vandenabeele P (2012) Many stimuli pull the necrotic trigger, an overview. Cell Death Differ 19:75–86
10. Galluzzi L, Vanden Berghe T, Vanlangenakker N, Buettner S, Eisenberg T, Vandenabeele P, Madeo F, Kroemer G (2011) Programmed necrosis from molecules to health and disease. Int Rev Cell Mol Biol 289:1–35
11. Degterev A, Huang Z, Boyce M, Li Y, Jagtap P, Mizushima N, Cuny GD, Mitchison TJ, Moskowitz MA, Yuan J (2005) Chemical inhibitor of nonapoptotic cell death with therapeutic potential for ischemic brain injury. Nat Chem Biol 1:112–119
12. Vitale I, Galluzzi L, Castedo M, Kroemer G (2011) Mitotic catastrophe: a mechanism for avoiding genomic instability. Nat Rev Mol Cell Biol 12:385–392
13. Ravichandran KS, Lorenz U (2007) Engulfment of apoptotic cells: signals for a good meal. Nat Rev Immunol 7:964–974
14. Vanden Berghe T, Vanlangenakker N, Parthoens E, Deckers W, Devos M, Festjens N, Guerin CJ, Brunk UT, Declercq W, Vandenabeele P (2010) Necroptosis, necrosis and secondary necrosis converge on similar cellular disintegration features. Cell Death Differ 17:922–930
15. Galluzzi L, Aaronson SA, Abrams J, Alnemri ES, Andrews DW, Baehrecke EH, Bazan NG, Blagosklonny MV, Blomgren K, Borner C, Bredesen DE, Brenner C, Castedo M, Cidlowski JA, Ciechanover A, Cohen GM, De Laurenzi V, De Maria R, Deshmukh M, Dynlacht BD, El-Deiry WS, Flavell RA, Fulda S, Garrido C, Golstein P, Gougeon ML, Green DR, Gronemeyer H, Hajnoczky G, Hardwick JM, Hengartner MO, Ichijo H, Jaattela M, Kepp O, Kimchi A, Klionsky DJ, Knight RA, Kornbluth S, Kumar S, Levine B, Lipton SA, Lugli E, Madeo F, Malomi W, Marine JC, Martin SJ, Medema JP, Mehlen P, Melino G, Moll UM, Morselli E, Nagata S, Nicholson DW, Nicotera P, Nunez G, Oren M, Penninger J, Pervaiz S, Peter ME, Piacentini M, Prehn JH, Puthalakath H, Rabinovich GA, Rizzuto R, Rodrigues CM, Rubinsztein DC, Rudel T, Scorrano L, Simon HU, Steller H, Tschopp J, Tsujimoto Y, Vandenabeele P, Vitale I, Vousden KH, Youle RJ, Yuan J, Zhivotovsky B, Kroemer G (2009) Guidelines for the use and interpretation of assays for monitoring cell death in higher eukaryotes. Cell Death Differ 16:1093–1107
16. Lotze MT, Tracey KJ (2005) High-mobility group box 1 protein (HMGB1): nuclear weapon in the immune arsenal. Nat Rev Immunol 5:331–342
17. Rovere-Querini P, Capobianco A, Scaffidi P, Valentinis B, Catalanotti F, Giazzon M, Dumitriu IE, Muller S, Iannacone M, Traversari C, Bianchi ME, Manfredi AA (2004) HMGB1 is an endogenous immune adjuvant released by necrotic cells. EMBO Rep 5:825–830
18. Scaffidi P, Misteli T, Bianchi ME (2002) Release of chromatin protein HMGB1 by necrotic cells triggers inflammation. Nature 418:191–195
19. Apetoh L, Ghiringhelli F, Tesniere A, Criollo A, Ortiz C, Lidereau R, Mariette C, Chaput N, Mira JP, Delaloge S, Andre F, Tursz T, Kroemer G, Zitvogel L (2007) The interaction between HMGB1 and TLR4 dictates the outcome of anticancer chemotherapy and radiotherapy. Immunol Rev 220:47–59
20. Zitvogel L, Kepp O, Kroemer G (2010) Decoding cell death signals in inflammation and immunity. Cell 140:798–804
21. Galluzzi L, Senovilla L, Zitvogel L, Kroemer G (2012) The secret ally: immunostimulation by anticancer drugs. Nat Rev Drug Discov 11:215–233
22. Michaud M, Martins I, Sukkurwala AQ, Adjemian S, Ma Y, Pellegatti P, Shen S, Kepp O, Scoazec M, Mignot G, Rello-Varona S, Tailler M, Menger L, Vacchelli E, Galluzzi L, Ghiringhelli F, di Virgilio F, Zitvogel L, Kroemer G (2011) Autophagy-dependent anticancer immune responses induced by chemotherapeutic agents in mice. Science 334:1573–1577